Evaluation of Geomorphic Descriptors Thresholds for Flood Prone Areas Detection on Ephemeral Streams in the Metropolitan Area of Bari (Italy)

Gabriella Balacco, Vincenzo Totaro(✉), Andrea Gioia, and Alberto Ferruccio Piccinni

Politecnico di Bari, Via E. Orabona, 470125 Bari, Italy
{gabriella.balacco, vincenzo.totaro, andrea.gioia, albertoferruccio.piccinni}@poliba.it

Abstract. Using geomorphic descriptors is a fast and reliable approach for mapping flood-prone areas exploiting Digital Elevation Models and their tools. However, calibration and validation procedures require a flooded map obtained by 1D/2D hydraulic simulation, which usually needs lots of information (available, for example, from remote sensing techniques) and important computational efforts. This approach is usually performed by calibration on a single event, using linear binary classifiers method and Receiver Operating Characteristics curves, in order to define an optimal threshold corresponding to a selected flooded map. On the other hand, the availability of flood-risk maps, provided by public or private institutions, is an important source of data for applying this procedure on a wide and hydrologically homogeneous area, in order to analyze some similitudes. In this study some interesting case studies located in Puglia region (Southern Italy) are investigated, using flooded maps for return periods of 30, 200 and 500 years provided by Basin Authority of Puglia; the aim of the proposed work is to compare the known flooded map areas with those obtained using several geomorphologic index on four case studies located in the metropolitan area of Bari (Puglia).

Keywords: Geomorphological descriptors · Flood-prone areas · DTM-based approach

1 Introduction

Puglia region (Southern Italy) is characterized by numerous shallow karst ephemeral/episodic streams locally known as "Lame". The deep fractured limestone that characterizes the western part of the middle of Puglia (called "Alta Murgia") ensures a high infiltration capacity and consequently this territory is characterized by the absence of a real and distinguishable drainage networks, except for several natural incisions. However, during extreme rainfall events, these streams are interested by significant flow rates that induce damages for assets and people.

© Springer Nature Switzerland AG 2019
S. Misra et al. (Eds.): ICCSA 2019, LNCS 11622, pp. 239–254, 2019.
https://doi.org/10.1007/978-3-030-24305-0_19

In the last years the increase of flood risk [1], as well as the observed changes in rainfall and flood frequency have generated the need of adapting traditional statistical tools for extreme events investigation and management [2–4]. Moreover, the increasing urbanization coupled with a decrement of vegetated areas may lead to the reduction of soil infiltration capacity with the consequent increasing of the frequency and significance of floods. Given the magnitude of the related consequences, the importance of accurate hazard evaluation and management is crucial not only in this field (e.g. [5]). In this way, decision-makers are aware of the need of developing appropriate actions useful to make safe people and assets from flood risk.

Several methodologies have been recently proposed for the investigation of the effects of a flood event (e.g. [6–13]) in the context of flood-prone areas delineation (e.g. [14–24]); these approaches need of hydrological and hydraulic data input, often scarcely available but essential for a reliable assessment.

In this direction, novel approaches, thanks to satellite products or earth observation images able to monitor spatial and temporal evolution of a territory, provide distributed information for hydraulic and/or hydrological applications (e.g. [25–31]), such as land use maps (e.g. [32–36]), stream network [37, 38], soil moisture condition (e.g. [39]) used for calibration/validation of hydrological models (e.g. [40, 41]) or building dataset (e.g. [42]). One of the most promising approaches is based on the basin geomorphology that permits to obtain useful data for determining the flood exposure.

Technical literature reported interesting results about the mutual relationship between floods and floodplain characteristics, that led to the proposition of simple methodologies which exploit geomorphic properties of river basins. (e.g. [43–47]).

Analyses reported in this work are carried out using a DEM-based methodology like that proposed by Samela et al. [22] and already tested by Gioia et al. [48] on a well-known ephemeral stream of central Puglia region. First results highlighted that this methodology is able to correlate the morphology of a basin with a certain extent of the floodplain, even if some of these descriptors are more suitable than others.

Regional analyses aim to extend at-site information to a wider area in order to make predictions for unmeasured locations [49, 50]. This is a relevant quality of these methods, because they can be very useful for large scale monitoring operations in several fields (e.g. [51]). Moving into this framework, we applied geomorphic descriptors on four case studies located in the metropolitan area of Bari (Puglia), looking for analogies or homogeneity in results.

2 Cases Study

Four case studies located in the metropolitan area of Bari (Puglia-Southern Italy) have been considered in this work. Their calibration domains are shown in Fig. 1.

Figure 2 shows the study areas inside a red outline, while stream networks are reported with a green line. Three different shades of blue have been used for representing the flooding maps corresponding to three design events characterized respectively by return periods of 30, 200 and 500 years. For the sake of clarity they have been extracted from the database of the Basin Authority of Puglia (http://webgis.adb.puglia.it/gis/map_default.phtml).

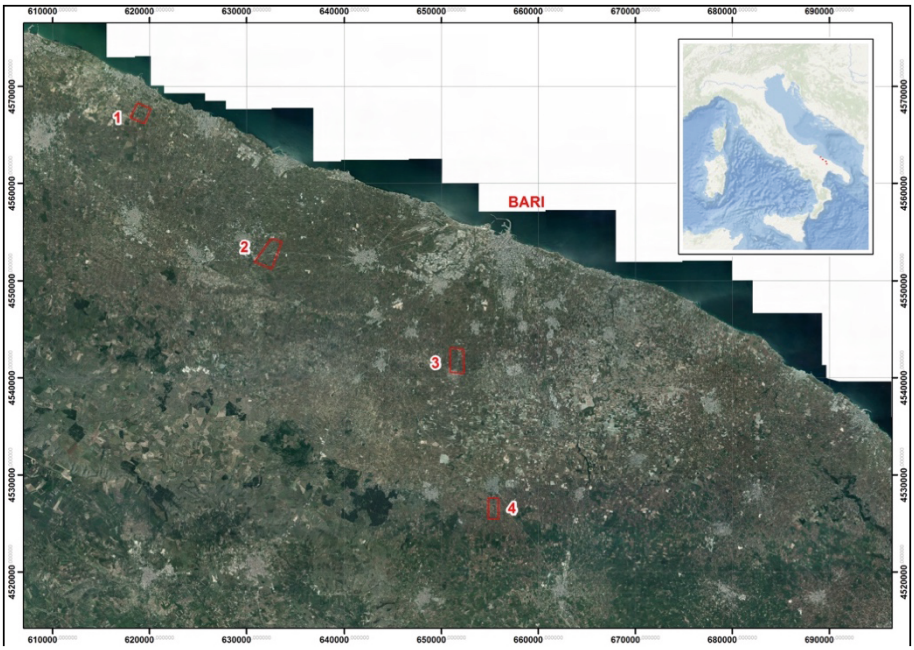

Fig. 1. Localization of the four study areas (in red) (Color figure online)

2.1 Study Area 1

Study area 1 is a part of a lama that originates in the municipality of Trani and, oriented in a SW-NE direction, slopes towards the sea crossing this territory. The stream extends for a length of approximately 5 km, with an estimated average slope of about 1.87%. The basin has an area of about 16 km^2 with altitudes ranging between 0 and 143 m.a.s.l.

This lama has a shallow morphological configuration crossing cultivated land with a total absence of incisions.

2.2 Study Area 2

Study area 2 is a part of the Martina lama (also known with the name of Cupa lama). It originates in Terlizzi at an elevation of about 210 m.a.s.l., where the stream network is not very recognizable and there is not a main riverbed. However, the main riverbed gradually becomes more pronounced proceeding downstream, assuming appreciable geomorphological significance already at the border of Molfetta. The outlet of this stream is located near the north-eastern area of Molfetta city.

The main reach of Martina lama extends for a length of approximately 17.6 km, with an estimated average slope of about 1.25%. The basin area, calculated at the mouth, reaches 25 km^2 with variable altitudes ranging between 0 and 224 m.a.s.l.

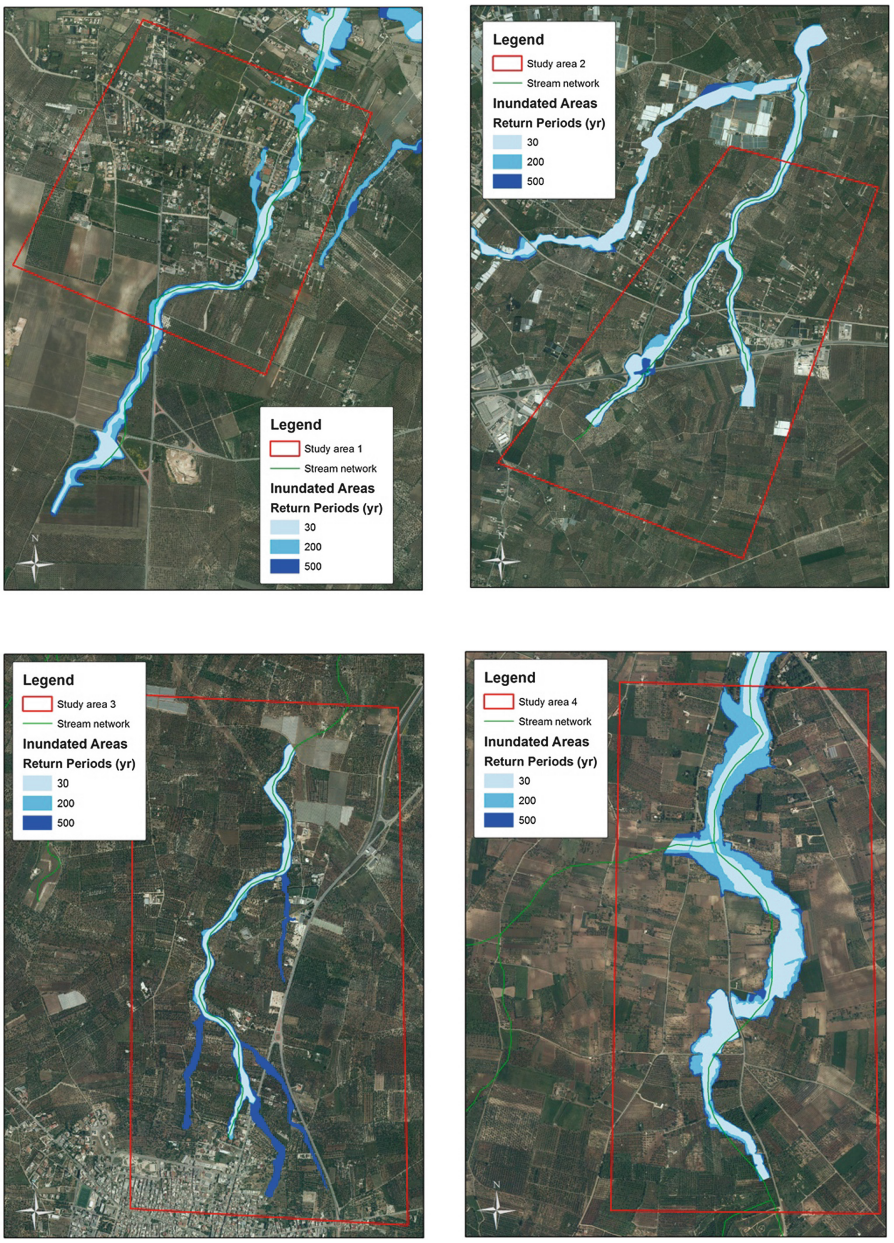

Fig. 2. Study areas.

2.3 Study Area 3

The study area identified as 3 concerns a portion of the hydrographic network of the Lamasinata lama, which is among the most important ephemeral streams of the metropolitan area of Bari. It originates between Palo del Colle and Bitetto and flowing through the land between Modugno and Bitritto reaches the industrial area of Bari. It flows approximately near the beach of S. Francesco-S. Cataldo, where it is still visible and is known as "canalone", built at the beginning of the twentieth century. The Lamasinata lama is characterized by a drainage area of about 370 km^2.

2.4 Study Area 4

This study area concerns a portion of the hydrographic network of Picone lama, which is the most important ephemeral stream that crosses the metropolitan area of Bari. It arises from the confluence of the Baronale stream, that flows through Adelfia, Loseto, Valenzano and Ceglie territories, and a second stream that originates from Sannicandro and flows through Loseto, Bitritto and Ceglie territories. The Picone lama, flowing in a SW-NE direction, reaches the city of Bari and finally flows into the sea together with Lamberti lama.

It has a drainage area of 292 km^2 and three different slope zones: a first section, very steep, with elevations above the 425 m.a.s.l.; follows a second zone, with elevations ranging between 425 and 325 m.a.s.l. characterized by a lower slope that connects to the final one, even less steep, which develops near the town of Bari.

There are historical evidences about floods occurred on the Picone lama as early as 1500; such events led the Duchess Isabella Sforza d'Aragona to undertake the construction of a channel outside the walls of the city, in order to canalize water during floods. However, in 1567 a flood destroyed these works, making the mouth of the lama even more unhealthy.

Since then many floods have occurred in Bari, due to significant rainfall events occurred on the Picone lama river basin, until in the early '900s a channel was built, to partially protect the city [52] by floods.

3 Methodologies

In the following the synthetic and composite geomorphological descriptors adopted for the evaluation of flood-prone areas, and the binary classifiers method, which allows to determine the best-performing descriptors are summarized. Receiver Operative Characteristics are mentioned in the last part of this section.

3.1 Morphological Descriptors of Basin

Geomorphic DEM-based descriptors are useful tools for appreciating the role of morphology on the evaluation of the susceptibility of areas to floods.

The model has been applied using a digital terrain model (DTM) with 8 m of resolution that was extracted from the territorial information system of Puglia Region (http://www.sit.puglia.it/).

There are different indices for evaluating flood prone areas, but the amount of data managed during the conducted analyses had led to describe only the four with the best performances.

Synthetic Descriptors

- *distance from the nearest stream, D [m]:* length of path connecting a cell on the grid with that hydrologically related on the drainage network;
- *elevation to the nearest stream, H [m]:* it is similar to *D*, but this index computes the elevation difference between the same points.

Composite Descriptors

- $ln(h_l/H)$: water depth h_l is an intrinsic cell quantity that can be defined as

$$h_l \cong bA_l^n \tag{1}$$

  where A_l [m^2] is the upslope contributing area for the selected cell, b is a scale factor usually set equal to 10^{-2} and n is a coefficient set equal to 0.3 [53].

- $ln(h_r/H)$ *Geomorphic Flood Index (GF)*: in this case, the upslope contributing area A_r [m^2] for the selected cell is related to that hydrologically connected on the stream network.

The ability of traditional indices in mapping flood prone areas has been tested using linear binary classifiers method [47]. The step-by-step procedure can be summarized as follows:

1. scaling and normalizing each map in the range between −1 and 1;
2. binary maps (*MOD*) are obtained applying a variable threshold to each normalized map with a step of 0.001. For each cell, the identifier 1 is assigned if flooded, 0 otherwise;
3. for each threshold step, a comparison with reference map (*REF*) has been done cell by cell, defining:
   - True Positive (TP): MOD(cell) and REF(cell) are both equal to 1;
   - False Positive (FP): MOD(cell) is 1 but REF(cell) is 0;
   - False Negative (FN): MOD(cell) is 0 and REF(cell) is 1;
   - True Negative (TN): MOD(cell) and REF(cell) are both equal to 0;

4. *true positive* and *false positive rate* are defined for each threshold as:

$$r_{tp} = \frac{TP}{TP + FN} \tag{2}$$

$$r_{fp} = \frac{FP}{FP + TN} \tag{3}$$

5. the best threshold (τ_{norm}) is defined minimizing the following objective function *OB:*

$$OB = r_{fp} + \left(1 - r_{tp}\right) \tag{4}$$

6. further considerations have been conducted plotting the whole series of r_{tp} and r_{fp} (i.e. the Receiver Operating Characteristics). Area under this curve is another tool which can give other useful information on the index performances.

4 Results and Discussion

The application of the procedure above described in Sect. 3, leads to the results reported in Tables 1, 2, 3 and 4. The ROC curves for a 200 years event are reported too in Figs. 3, 4, 5 and 6. In Fig. 7 flooded areas for a 200 years event and for H descriptors are shown.

Table 1. Results of the linear binary classification test for the Area 1

	Indices	τ_{norm}	r_{fp}	r_{tp}	*min*(OB)	AUC
30 years	D	−0.869	0.256	0.909	0.347	0.906
	H	−0.898	0.125	0.845	0.280	0.938
	GFI	−0.523	0.184	0.923	0.261	0.943
	$\ln(h_l/H)$	−0.535	0.196	0.895	0.302	0.930
200 years	D	−0.886	0.191	0.795	0.396	0.862
	H	−0.862	0.137	0.812	0.325	0.888
	GFI	−0.523	0.145	0.845	0.301	0.893
	$\ln(h_l/H)$	−0.543	0.173	0.805	0.368	0.885
500 years	D	−0.886	0.182	0.799	0.383	0.866
	H	−0.862	0.127	0.814	0.313	0.889
	GFI	−0.523	0.135	0.844	0.291	0.893
	$\ln(h_l/H)$	−0.544	0.165	0.804	0.361	0.887

Table 2. Results of the linear binary classification test for the Area 2

	Indices	τ_{norm}	r_{fp}	r_{tp}	*min*(OB)	AUC
30 years	D	−0.821	0.191	0.866	0.325	0.919
	H	−0.790	0.162	0.917	0.245	0.938
	GFI	−0.444	0.128	0.887	0.241	0.933
	$\ln(h_l/H)$	−0.503	0.160	0.866	0.294	0.923
200 years	D	−0.794	0.225	0.874	0.351	0.906
	H	−0.790	0.147	0.867	0.280	0.923
	GFI	−0.475	0.144	0.861	0.284	0.913
	$\ln(h_l/H)$	−0.516	0.164	0.829	0.335	0.901
500 years	D	−0.794	0.206	0.869	0.337	0.909
	H	−0.773	0.150	0.867	0.283	0.919
	GFI	−0.474	0.126	0.834	0.292	0.907
	$\ln(h_l/H)$	−0.526	0.163	0.812	0.351	0.891

Table 3. Results of the linear binary classification test for the Area 3

	Indices	τ_{norm}	r_{fp}	r_{tp}	*min*(OB)	AUC
30 years	D	−0.913	0.138	0.903	0.235	0.946
	H	−0.859	0.152	0.957	0.194	0.948
	GFI	−0.366	0.122	0.950	0.172	0.958
	$\ln(h_l/H)$	−0.447	0.144	0.919	0.225	0.943
200 years	D	−0.898	0.160	0.925	0.235	0.944
	H	−0.849	0.157	0.943	0.214	0.942
	GFI	−0.390	0.130	0.942	0.188	0.954
	$\ln(h_l/H)$	−0.447	0.138	0.889	0.249	0.935
500 years	D	−0.887	0.154	0.773	0.381	0.876
	H	−0.806	0.166	0.829	0.337	0.902
	GFI	−0.411	0.114	0.754	0.360	0.885
	$\ln(h_l/H)$	−0.506	0.156	0.812	0.344	0.903

The first observation arises by looking at the shape of flooded areas (Fig. 2): in fact, a simple visual inspection of areas 2 and 4 shows that they are very similar for the three investigated return periods; this reflects on the performances of the indexes, which are similar (but not equal) in terms of minimum of the objective function. More in detail, if we look at the objective function, H is always the best performant descriptors, except in few cases (where GFI is slightly better).

Table 4. Results of the linear binary classification test for the Area 4

	Indices	τ_{norm}	r_{fp}	r_{tp}	*min*(OB)	AUC
30 years	D	−0.765	0.208	0.803	0.405	0.890
	H	−0.845	0.129	0.861	0.268	0.934
	GFI	−0.506	0.124	0.848	0.276	0.930
	$\ln(h_l/H)$	−0.570	0.213	0.930	0.283	0.929
200 years	D	−0.725	0.240	0.838	0.402	0.887
	H	−0.829	0.112	0.884	0.229	0.952
	GFI	−0.524	0.106	0.871	0.235	0.948
	$\ln(h_l/H)$	−0.574	0.188	0.931	0.257	0.944
500 years	D	−0.709	0.252	0.856	0.396	0.890
	H	−0.829	0.099	0.876	0.223	0.955
	GFI	−0.539	0.108	0.877	0.231	0.951
	$\ln(h_l/H)$	−0.574	0.175	0.923	0.252	0.946

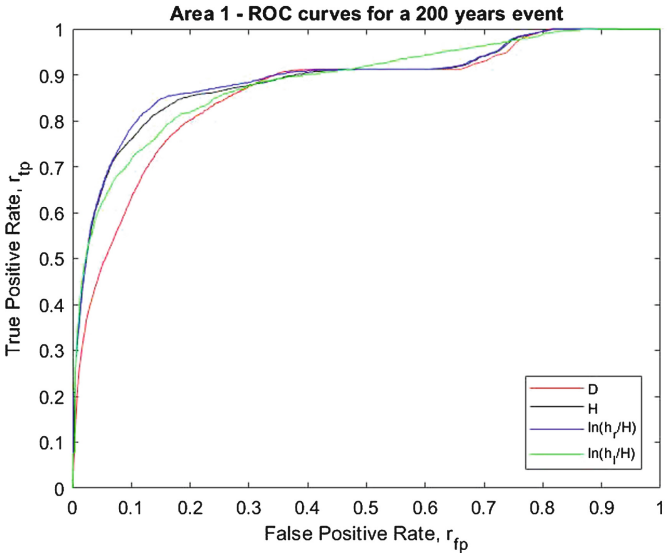

Fig. 3. ROC curves for a 200 years flood event for Area 1

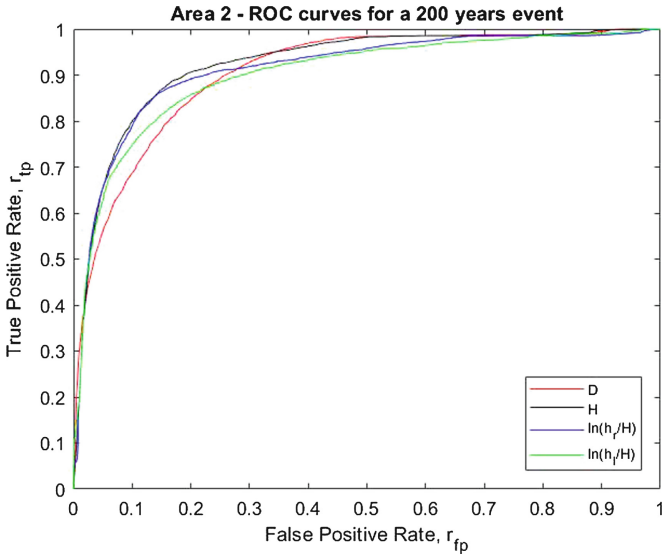

Fig. 4. ROC curves for a 200 years flood event for Area 2

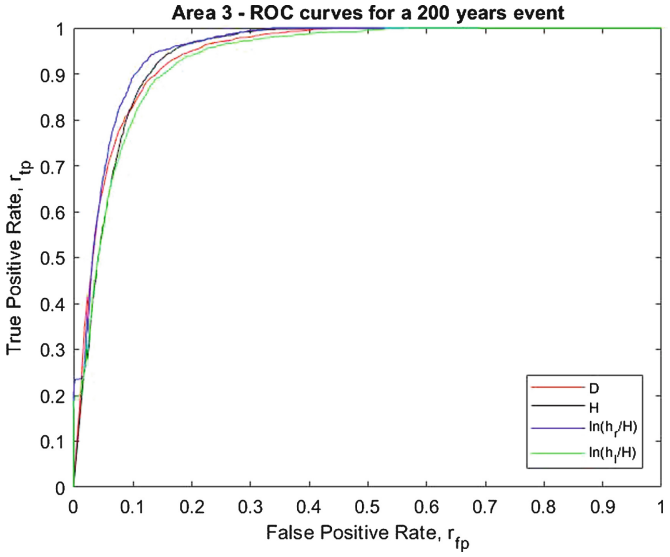

Fig. 5. ROC curves for a 200 years flood event for Area 3

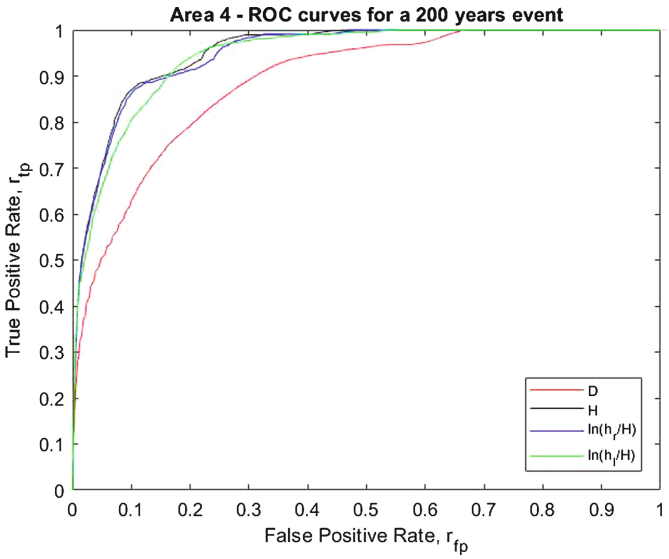

Fig. 6. ROC curves for a 200 years flood event for Area 4

Areas 1 and 3 are affected by a modification in the structure of flooded area: in fact, looking at the Fig. 2, in area 1 a secondary stream is activated for a return period greater than 200 years. The main consequence is that an increasing in the minimum of the objective function. Secondary streams are also activated for a return period of 500 years, generating a not significant lost in performances bot in the minimum of the OB and in the AUC: this can be related to a homogeneous distribution of morphology in the river stream.

An interesting observation arises from the previous tables, and it concerns with the GFI false positive rate which is, except in a few cases, that with the lowest value. This can reveal an ability of this descriptor to represent a good indicator for flood-prone areas delineation. A more complex situation for the true positive rate can be reported too.

Finally, it can be useful to remark that the particular distribution of flooded areas (which are similar for the three return periods analyzed) reflects on the values of the normalized thresholds: in fact, a reduced difference with the increasing of return period has been found. This is coherent with the theoretical framework which underlies this approach.

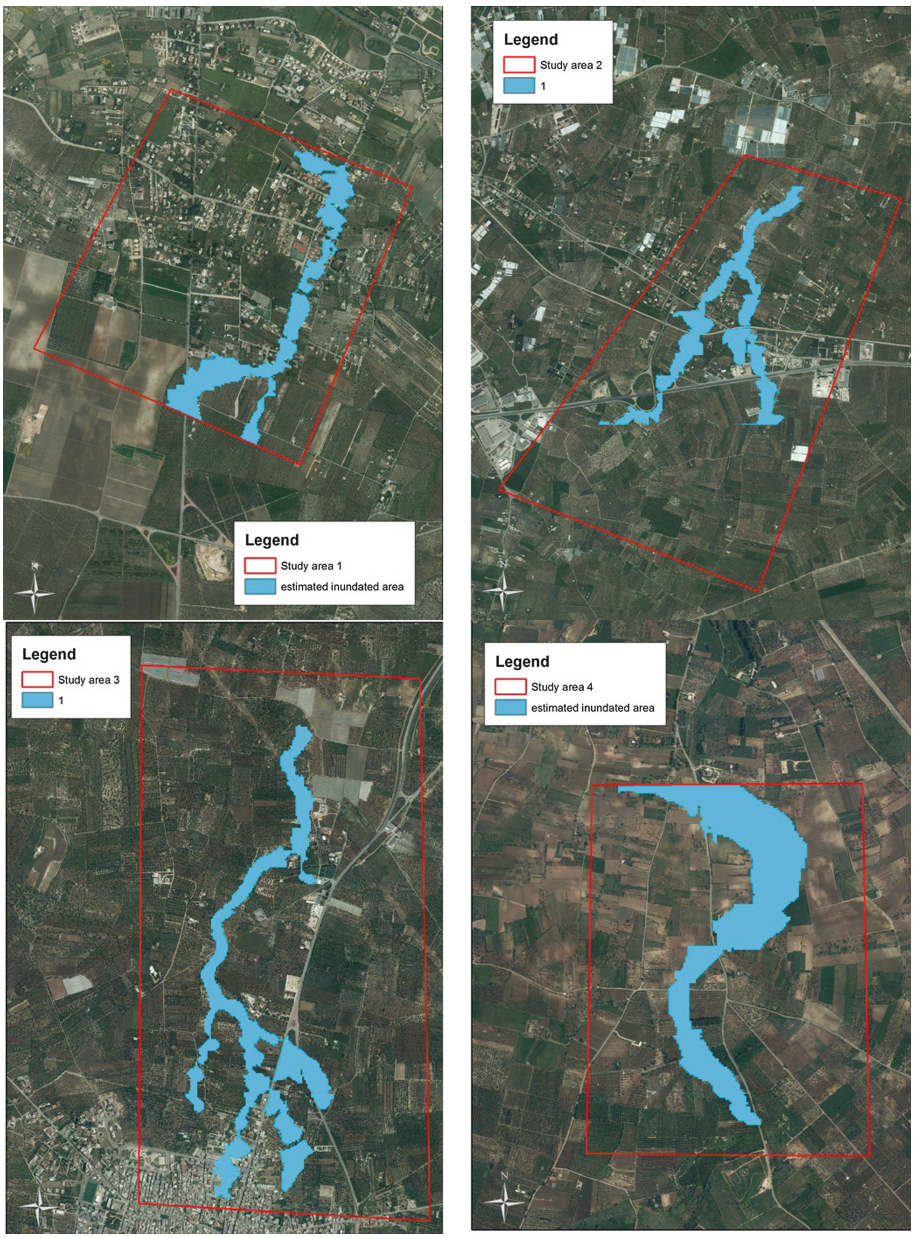

Fig. 7. Area exposed to flood inundation identified by the descriptor H for a 200 years event

5 Conclusions

The application of geomorphic descriptors to four ephemeral streams located in a small area in the district of Bari (southern Italy) has been shown in this work. The hydraulic complexity of this kind of streams and the singularity of the morphology in surrounding areas are the two main factor that, in our opinion, may influence the spatial distribution of flooded areas. The first observation that arises is the substantial analogy of geomorphological descriptors performances in the cases of similar reference flooded areas, while there is a different behavior when secondary streams are activated. The most important role, in this case, can be played by the local morphology, which can lead to a redistribution of flood that cannot be recognized by descriptors. Their ability in detecting flooded areas can be influenced, moreover, by a compromise between a wide flooded area and the value of the thresholds. However, the performances of the investigated indicators are globally good. This study can confirm the importance of the availability of fast and rapid tools for a preliminary definition of flood risk maps at regional scale.

It is interesting to point out that the DTM resolution may influence this kind of analyses; in this context an interesting detection of extended study areas and the DTM resolution effects on the descriptor performances, may be conducted in future works.

Extending case studies to other ephemeral streams located in different study areas can be an important step for understanding not only their behavior with DTM based methods, but also for improving the degree of knowledge of these steams.

References

1. Milly, P.C.D., Wetherald, R.T., Dunne, K.A., Delworth, T.L.: Increasing risk of great floods in a changing climate. Nature **415**(6871), 514 (2002)
2. Salas, J.D., Obeysekera, J.: Revisiting the concepts of return period and risk for nonstationary hydrologic extreme events. J. Hydrol. Eng. **19**(3), 554–568 (2013)
3. De Paola, F., Giugni, M., Pugliese, F., Annis, A., Nardi, F.: GEV parameter estimation and stationary vs. non-stationary analysis of extreme rainfall in African test cities. Hydrology **5**(2), 28 (2018)
4. Obeysekera, J., Salas, J.D.: Quantifying the uncertainty of design floods under nonstationary conditions. J. Hydrol. Eng. **19**(7), 1438–1446 (2013)
5. Sangiorgio, V., Uva, G., Fatiguso, F.: Optimized AHP to overcome limits in weight calculation: building performance application. J. Constr. Eng. Manage. **144**(2), 04017101 (2017)
6. Ignacio, J.A.F., Cruz, G.T., Nardi, F., Henry, S.: Assessing the effectiveness of a social vulnerability index in predicting heterogeneity in the impacts of natural hazards: case study of the Tropical Storm Washi flood in the Philippines. Vienna Yearb. Popul. Res. **13**(1), 91–130 (2015)
7. Feldman, A.D.: Hydrologic Engineering Center (U.S.), Hydrologic Modeling System HEC-HMS, US Army Corps of Engineers, Hydrologic Engineering Center (2000)
8. Fiorentino, M., Gioia, A., Iacobellis, V., Manfreda, S.: Analysis on flood generation processes by means of a continuous simulation model. Adv. Geosci. **7**, 231–236 (2006). ISSN 1680-7340

9. Merz, R., Blöschl, G.: Flood frequency hydrology: 1. Temporal, spatial, and causal expansion of information. Water Resour. Res. **44**, W08432 (2008). https://doi.org/10.1029/2007WR006744
10. Iacobellis, V., Fiorentino, M., Gioia, A., Manfreda, S.: Best fit selection of theoretical flood frequency distributions based on different runoff generation mechanisms. Water **2**(2, 1), 239–256 (2010)
11. Beven, K.: Rainfall-Runoff Modelling. The Primer, 2nd edn. Wiley-Blackwell, Chichester (2012)
12. Gioia, A., Manfreda, S., Iacobellis, V., Fiorentino, M.: Performance of a theoretical model for the description of water balance and runoff dynamics in southern Italy. J. Hydrol. Eng. **19**(6), 1113–1123 (2014)
13. Di Modugno, M., et al.: Build-up/wash-off monitoring and assessment for sustainable management of first flush in an urban area. Sustainability **7**, 5050–5070 (2015)
14. Gioia, A., Iacobellis, V., Manfreda, S., Fiorentino, M.: Comparison of different methods describing the peak runoff contributing areas during floods. Hydrol. Process. **31**(11), 2041–2049 (2017)
15. De Wrachien, D., Mambretti, S.: Mathematical models for flood hazard assessment. Int. J. Saf. Secur. Eng. **1**(4), 353–362 (2011)
16. Iacobellis, V., Castorani, A., Di Santo, A.R., Gioia, A.: Rationale for flood prediction in karst endorheic areas. J. Arid Environ. **112**(PA), 98–108 (2015)
17. Bates, P., Anderson, M., Price, D., Hardy, R., Smith, C.: Analysis and development of hydraulic models for floodplain flows. In: Anderson, M.G., Walling, D.E., Bates, P.D. (eds.) Floodplain Processes. Wiley, New York (1996)
18. Aronica, G., Hankin, B., Beven, K.J.: Uncertainty and equifinality in calibrating distributed roughness coefficients in a flood propagation model with limited data. Adv. Water Resour. **22**(4), 349–365 (1998)
19. Jain, S.K., Singh, R.D., Jain, M.K., Lohani, A.K.: Delineation of flood-prone areas using remote sensing techniques. Water Resour. Manage. **19**(4), 333–347 (2005)
20. Fluet-Chouinard, E., Lehner, B., Rebelo, L.M., Papa, F., Hamilton, S.K.: Development of a global inundation map at high spatial resolution from topographic downscaling of coarse-scale remote sensing data. Remote Sens. Environ. **158**, 348–361 (2015)
21. Peña, F., Nardi, F.: Floodplain terrain analysis for coarse resolution 2D flood modeling. Hydrology **5**(4), 52 (2018)
22. Manfreda, S., et al.: Flood-prone areas assessment using linear binary classifiers based on flood maps obtained from 1D and 2D hydraulic models. Nat. Hazards **79**(2), 735–754 (2015)
23. Iacobellis, V., et al.: Investigation of a flood event occurred on lama Balice, in the context of hazard map evaluation in karstic-ephemeral streams. In: Gervasi, O., et al. (eds.) ICCSA 2018. LNCS, vol. 10964, pp. 317–333. Springer, Cham (2018). https://doi.org/10.1007/978-3-319-95174-4_26
24. Totaro, V., Gioia, A., Novelli, A., Caradonna, G.: The use of geomorphological descriptors and Landsat-8 spectral indices data for flood areas evaluation: a case study of Lato river basin. In: Gervasi, O., et al. (eds.) ICCSA 2017. LNCS, vol. 10407, pp. 30–44. Springer, Cham (2017). https://doi.org/10.1007/978-3-319-62401-3_3
25. Totaro, V., Peschechera, G., Gioia, A., Iacobellis, V., Fratino, U., Tarantino, E.: Comparison of satellite and geomorphic indices for flooded areas detection in a Mediterranean river basin (in preparation)
26. Bates, P.D., Horritt, M.S., Smith, C.N., Mason, D.C.: Integrating remote sensing observations of flood hydrology and hydraulic modelling. Hydrol. Process. **11**, 1777–1795 (1997)

27. Horritt, M.S., Mason, D.C., Luckman, A.J.: Flood boundary delineation from synthetic aperture radar imagery using a statistical active contour model. Int. J. Remote Sens. **22**(13), 2489–2507 (2001)
28. Mattia, F., et al.: Time series of COSMO-SkyMed data for landcover classification and surface parameter retrieval over agricultural sites. In: Proceedings of the IEEE 2012 International Geoscience and Remote Sensing Symposium, pp. 6511–6514 (2012). ISBN 978-1-4673-1159-5
29. Balenzano, A., et al.: On the use of multi-temporal series of COSMO-SkyMed data for landcover classification and surface parameter retrieval over agricultural sites. In: Proceedings of the 2011 IEEE International Geoscience and Remote Sensing Symposium, 24–29 July 2011, Vancouver, Canada, pp. 142–145 (2011)
30. Balenzano, A., et al.: A ground network for SAR-derived soil moisture product calibration, validation and exploitation in southern Italy. In: Proceedings of the IEEE 2014 International Geoscience and Remote Sensing Symposium, IGARSS 2014 (2014)
31. Tarantino, E., Novelli, A., Laterza, M., Gioia, A.: Testing high spatial resolution WorldView-2 imagery for retrieving the leaf area index. In: Third International Conference on Remote Sensing and Geoinformation of the Environment (RSCy2015), vol. 9535, p. 95351N. International Society for Optics and Photonics (2015)
32. Trombetta, A., Iacobellis, V., Tarantino, E., Gentile, F.: Calibration of the AquaCrop model for winter wheat using MODIS LAI images. Agric. Water Manag. **164**(Part 2), 304–316 (2016)
33. Olang, L.O., Kundu, P., Bauer, T., Fürst, J.: Analysis of spatio-temporal land cover changes for hydrological impact assessment within the Nyando River Basin of Kenya. Environ. Monit. Assess. **179**, 389–401 (2011)
34. Pattison, I., Lane, S.N.: The link between land-use management and fluvial flood risk: a chaotic conception? Prog. Phys. Geogr. **36**, 72–92 (2011)
35. Balacco, G., Figorito, B., Tarantino, E., Gioia, A., Iacobellis, V.: Space-time LAI variability in Northern Puglia (Italy) from SPOT VGT data. Environ. Monit. Assess. **187**, 434 (2015)
36. Caprioli, M., Tarantino, E.: Identification of land cover alterations in the Alta Murgia National Park (Italy) with VHR satellite imagery. Int. J. Sustain. Dev. Plan. **1**(3), 261–270 (2006)
37. Crocetto, N., Tarantino, E.: A class-oriented strategy for features extraction from multidate ASTER imagery. Remote Sens. **1**(4), 1171–1189 (2009)
38. Fidelibus, M.D., Balacco, G., Gioia, A., Iacobellis, V., Spilotro, G.: Mass transport triggered by heavy rainfall: the role of endorheic basins and epikarst in a regional karst aquifer. Hydrol. Process. **31**(2), 394–408 (2017)
39. Figorito, B., Tarantino, E., Balacco, G., Fratino, U.: An object-based method for mapping ephemeral river areas from WorldView-2 satellite data. In: Remote Sensing for Agriculture, Ecosystems, and Hydrology XIV, vol. 8531, p. 85310B. International Society for Optics and Photonics (2012)
40. Saradjian, M.R., Hosseini, M.: Soil moisture estimation by using multipolarization SAR image. Adv. Space Res. **48**(2), 278–286 (2011)
41. Iacobellis, V., Gioia, A., Milella, P., Satalino, G., Balenzano, A., Mattia, F.: Inter-comparison of hydrological model simulations with time series of SAR-derived soil moisture maps. Eur. J. Remote Sens. **46**(1), 739–757 (2013)
42. Peschechera, G., Fratino, U.: Calibration of CLAIR model by means of Sentinel-2 LAI data for analysing wheat crops through Landsat-8 surface reflectance data. In: Gervasi, O., et al. (eds.) ICCSA 2018. LNCS, vol. 10964, pp. 294–304. Springer, Cham (2018). https://doi.org/10.1007/978-3-319-95174-4_24

43. Gioia, A., Iacobellis, V., Manfreda, S., Fiorentino, M.: Influence of infiltration and soil storage capacity on the skewness of the annual maximum flood peaks in a theoretically derived distribution. Hydrol. Earth Syst. Sci. **16**, 937–951 (2012)
44. Williams, W.A., Jensen, M.E., Winne, J.C., Redmond, R.L.: An automated technique for delineating and characterizing valley-bottom settings. Environ. Monit. Assess. **64**(1), 105–114 (2000)
45. Gallant, J.C., Dowling, T.I.: A multiresolution index of valley bottom flatness for mapping depositional areas. Water Resour. Res. **39**(12), 1347 (2003). https://doi.org/10.1029/2002WR001426
46. Nardi, F., Vivoni, E.R., Grimaldi, S.: Investigating a floodplain scaling relation using a hydrogeomorphic delineation method. Water Resour. Res. **42**, W09409 (2006). https://doi.org/10.1029/2005WR004155
47. Manfreda, S., Di Leo, M., Sole, A.: Detection of flood prone areas using digital elevation models. J. Hydrol. Eng. **16**(10), 781–790 (2011)
48. Samela, C., Manfreda, S., Paola, F.D., Giugni, M., Sole, A., Fiorentino, M.: DEM-based approaches for the delineation of flood-prone areas in an ungauged basin in Africa. J. Hydrol. Eng. **21**(2), 06015010 (2015)
49. Gioia, A., Totaro, V., Bonelli, R., Esposito, A.A.M.G., Balacco, G., Iacobellis, V.: Flood susceptibility evaluation on ephemeral streams of Southern Italy: a case study of lama Balice. In: Gervasi, O., et al. (eds.) ICCSA 2018. LNCS, vol. 10964, pp. 334–348. Springer, Cham (2018). https://doi.org/10.1007/978-3-319-95174-4_27
50. Cunnane, C.: Methods and merits of regional flood frequency analysis. J. Hydrol. **100**(1–3), 269–290 (1988)
51. Fiorentino, M., Gioia, A., Iacobellis, V., Manfreda, S.: Regional analysis of runoff thresholds behaviour in Southern Italy based on theoretically derived distributions. Adv. Geosci. **26**, 139–144 (2011)
52. Sangiorgio, V., Uva, G., Fatiguso, F.: User reporting–based semeiotic assessment of existing building stock at the regional scale. J. Perform. Constr. Facil. **32**(6), 04018079 (2018)
53. Mossa, M.: The floods in Bari: what history should have taught. J. Hydraul. Res. **45**(5), 579–594 (2007)